Earth Planets Space, **65**, 749–757, 2013

Delineation of the subsurface structures and basement surface of the Abu-Rodaym area, Southwestern Sinai, using ground magnetic data

Hatem Aboelkhair[1] and Mostafa Rabei[2]

[1]*Geology Department, Faculty of Science, Damietta University, New Damietta, Egypt*
[2]*Expbration Division, Nuclear Materials Authority, Cairo, Egypt*

(Received January 24, 2012; Revised December 3, 2012; Accepted December 17, 2012; Online published August 23, 2013)

The present study deals with the analysis of data from a ground magnetic survey that was conducted in the Abu-Rodaym area of the Southwestern Sinai Peninsula, Egypt. This survey was carried out to delineate the subsurface structural framework, and to identify the thickness of the sedimentary basin of the study area. Locating these structures, and determining the localities of maximum sedimentary thicknesses that consist mainly of sandstone, serves as a preliminary process in exploring the confined aquifer beneath the surface of the Abu-Rodaym area. This will greatly benefit Bedouins who suffer greatly from a lack of water in the driest region in the country. The processing, analysis, and interpretation, of the total intensity magnetic data shows that there are three sets of faults striking mainly in the N-S, NW-SE, and NE-SW, directions. The depth to the basement surface was found to fluctuate from about 45 m, to more than 100 m, beneath the ground surface. It was also found that the variations in magnetic observations were produced by the striking structures that are mainly responsible for the variations in thicknesses of the sedimentary rocks in the area.
Key words: Ground magnetic, groundwater, sedimentary basin, Basement, Sinai, Egypt.

1. Introduction

The Sinai peninsula (Fig. 1) is surrounded by the Mediterranean Sea in the north, the Red Sea in the south, and is enclosed by the two spectacular branches of the African Rift Valley—the Gulf of Aqaba in the west and the Gulf of Suez in the east—and is a unique region in the world. The peninsula can conveniently be divided into a northern and a southern region. The northern part consists of flat-lying Paleozoic, and more recent, sediments, while the southern part consists essentially of metamorphic and magmatic rocks of Pre-Cambrian age. This southern portion is a continuation of the Arabian-Nubian Desert. The study area is located between latitudes (29°06′28″ and 29°07′2″)N and longitudes (33°19′10″ and 33°20′40″)E covering an area of about 2 km^2 near the western part of the Abu-Rodaym region at the northeastern part of Abu Zeneima city in the Southwestern (SW) Sinai Peninsula (Fig. 1).

A magnetic survey is a powerful tool for delineating the geology (lithology and subsurface structure) of buried basement terrain. Such a survey maps the variation of the geomagnetic field, which occurs due to changes in the percentage of magnetite in the rock. It reflects the variations in the distribution and type of magnetic minerals below the Earth's surface (Mekonnen, 2004). Magnetic minerals can be mapped from the surface to greater depths in the rock crust depending on the dimension, shape, and magnetic property, of the rock. Sedimentary formations are usually nonmagnetic and, consequently, have little effect, whereas mafic and ultramafic igneous rocks exhibit a greater variation and are useful in exploring the bedrock geology concealed below cover formations (Mekonnen, 2004).

The main objectives of this study are to delineate the trends of the subsurface structures, to determine the depth to the basement surface, and to study the groundwater potentialities of the study area.

To achieve these goals, a ground magnetic survey of the Abu-Rodaym area was conducted. The magnetic survey data were subjected to a quantitative interpretation that involved some geophysical processing and interpretational techniques, including: (1) reducing the total intensity magnetic data to the north magnetic pole; (2) isolating the magnetic data into their residual, and regional, components, using Fast Fourier Transformation (FFT) techniques; (3) Euler deconvolution to delineate the subsurface structures from the RTP regional magnetic map; and (4) two-dimensional magnetic forward modeling along two selected RTP magnetic profiles.

2. Geologic Setting

Structurally, the southwestern part of Sinai is strongly tectonized where faults, folds, as well as joints, are the main structural features. El Rakaiby and El Aassy (1990) concluded that the N-S, ENE-WSW, NE-SW and NNW-SSE are the main fault trends in the Um Bogma area. Al Shami (1994) studied the main structural setting of Wadi Allouga at the South of the Abu-Rodaym area and concluded that the area was subjected to two phases of compressional forces; the older of these was acting in the E-W direction, while the

doi:10.5047/eps.2012.12.006

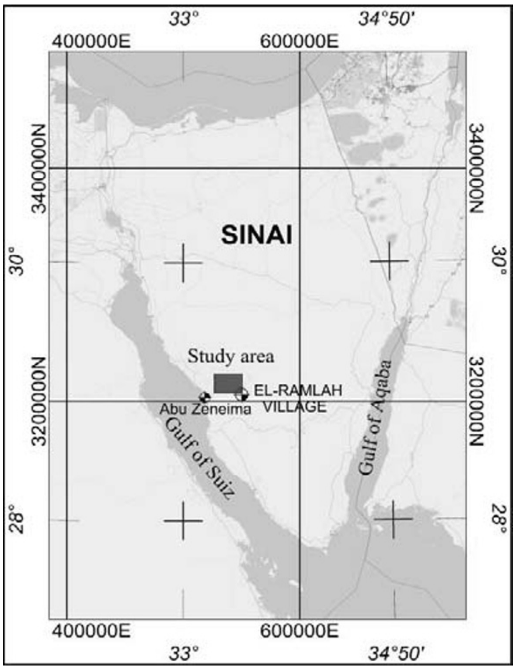

Fig. 1. Location map of the Abu-Rodaym area, Southwestern Sinai, Egypt.

more recent was acting in the N-S direction. He added that these structural features played the most important role in the mode of occurrence of radioactive mineralization in this area.

Al-Shami (2003) classified the lithologic succession of Paleozoic rocks that cover the study area into seven formations arranged from the oldest; the Sarabit El-Khadim, Abu-Hamata and Adadia Formations (the so-called "lower sandstone series"). This is followed unconformably upwards by the Um-Bogma Formation (the "Carboniferous limestone series"), and overlain by the El-Hashash, Magharet El-Mayah, and Abu-Zarab Formations, which represent the Abu-Thora formation according to Kora (1984), or the "upper sandstone series" by Barron (1907).

The geologic map of the study area (Fig. 2) shows that the Abu-Thora Formation occupies about 15% of the study area's surface, and is mainly sited in scattered localities in its northern part. In addition, Quaternary sediments occupy about 85% of the surface of the study area and can be divided into two categories according to their lithological constituents: clayey deposits that represent a semi-consolidated layer having a large amount of clay menials; and sandy deposits that represent unconsolidated deposits having a large amount of sands.

3. Magnetic Data Acquisition and Survey Design

The proton precession magnetometer (model PMG-1) was used in the present survey in order to generate the measurements of the total magnetic intensity of the Earth. The ground magnetic survey in the Abu-Rodaym area was accomplished on a grid pattern parallel to the north-south direction (Fig. 3), with a station interval of about 20 m and a line interval of about 40 m. The roving PMG-1 magnetometer was set up to a single mode and, at the same time, another fixed PMG-1 was set up to an auto mode in order to measure the total magnetic intensity field every 30 seconds, as a base station, in order to correct the diurnal variations in the total magnetic field.

4. Magnetic Data Processing

The processing techniques, including spectral analysis, were applied. The data processing passed through various steps, starting by converting the corrected TMI data from the space domain to a frequency domain, using Fast Fourier Transformation (FFT). Then, the reduction to the north magnetic pole (RTP) map was derived from the total mag-

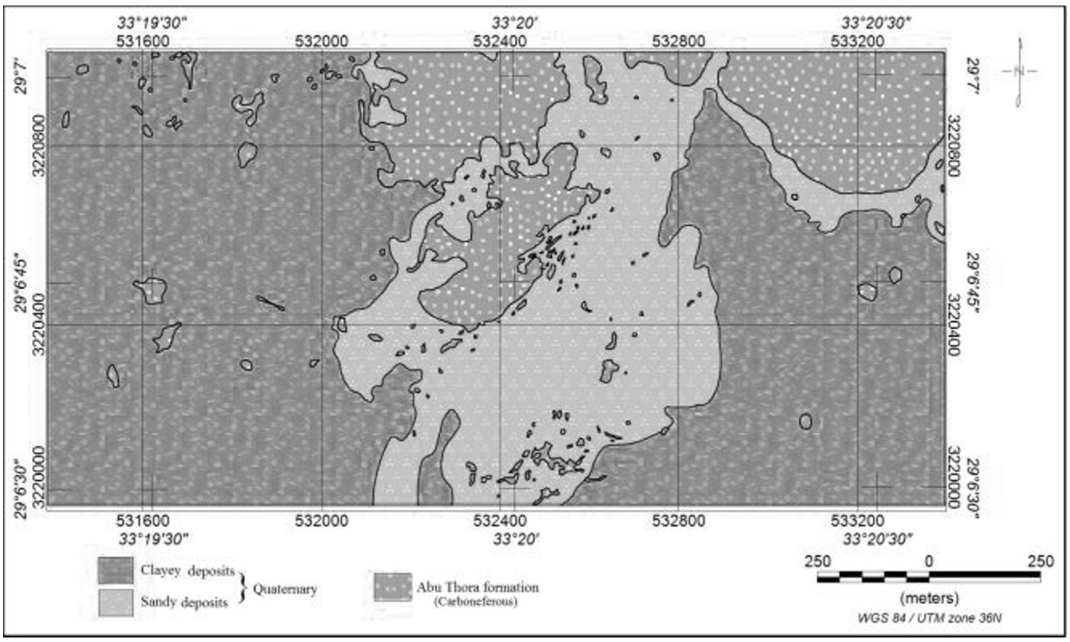

Fig. 2. The geologic map of the Abu-Rodaym area, Southwestern Sinai, Egypt.

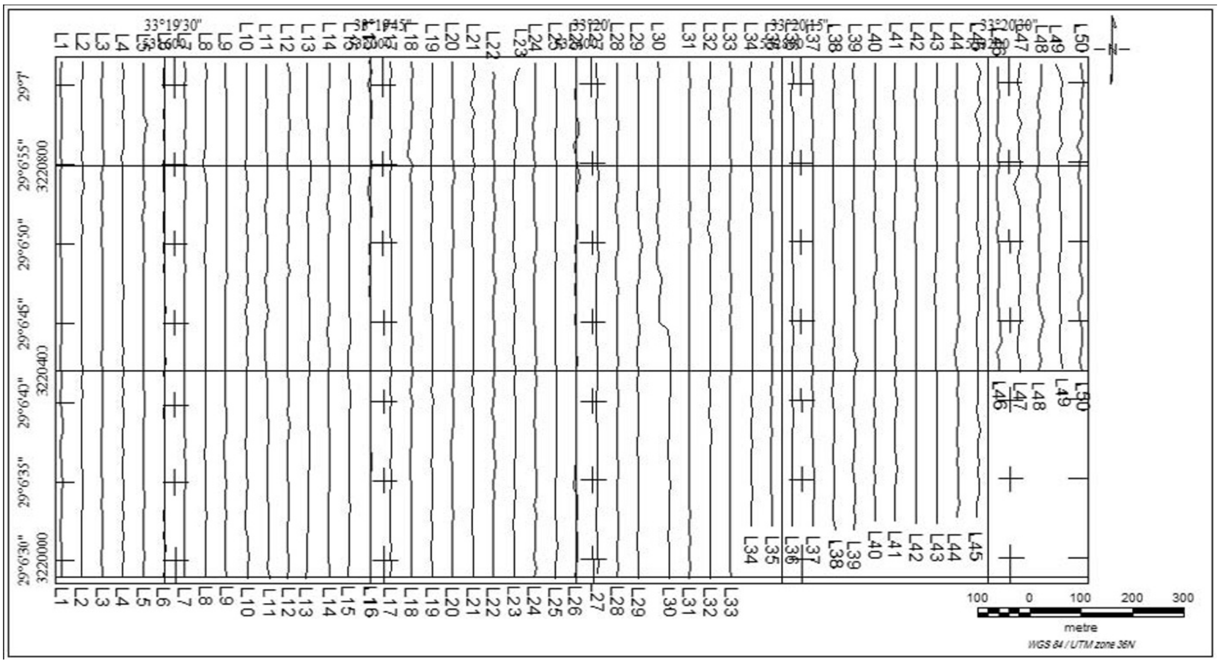

Fig. 3. Location map of the survey lines of land magnetic observations of the study area.

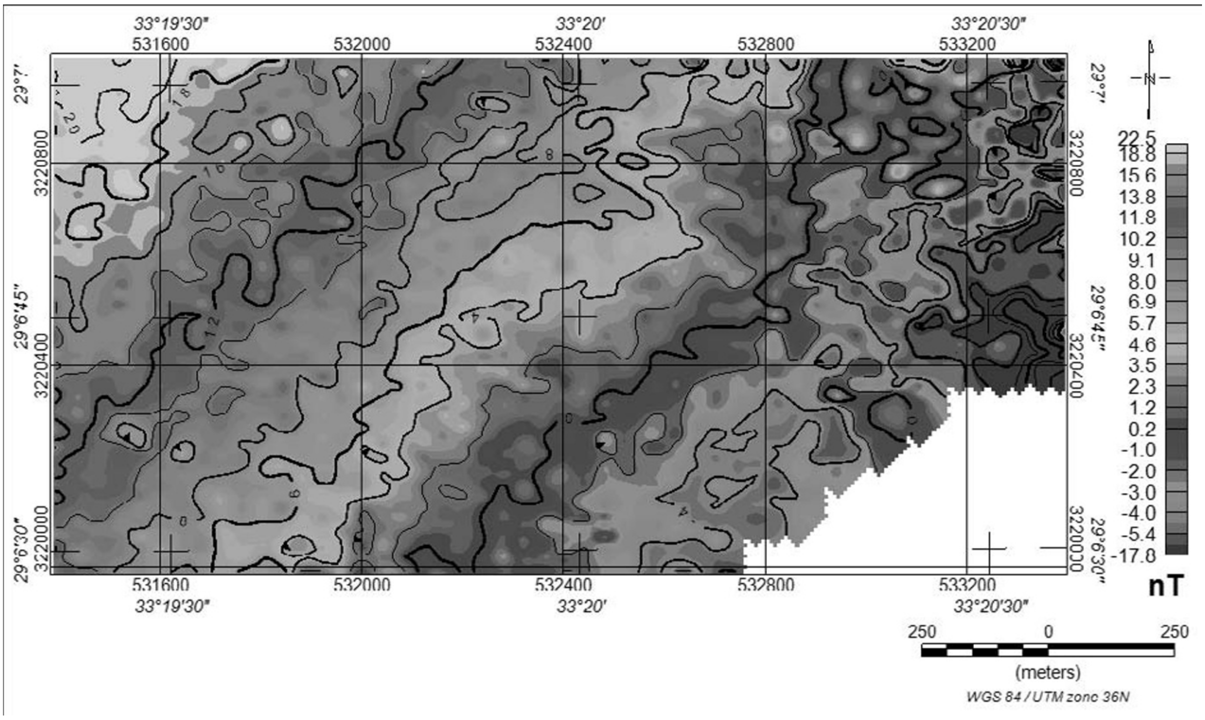

Fig. 4. Total intensity magnetic map of the Abu-Rodaym area. C.I. = nT.

netic intensity data, using inclination and declination values of 44.3° and 2.45°, respectively (Rabie, 2011).

After applying all the corrections to the observed magnetic data, the total intensity magnetic data of the study area were gridded and contoured using the Oasis montaj 7.0.1 package (Geosoft, 2007) in order to create the total intensity magnetic map (TIM), and then the International Geomagnetic Reference Field (IGRF) was removed (Fig. 4).

5. Reduction to the Pole (RTP)

Reduction to the pole transforms an anomaly into the anomaly that would have been observed if the magnetization and regional field were vertical (as if the anomaly was measured at the north magnetic pole). A symmetric body produces a symmetric anomaly at the magnetic poles. Hence, reduction to the pole is a way to remove the asymmetries caused by a non-vertical magnetization, or regional field, and to produce a simpler set of anomalies to interpret (Dobrin and Savit, 1988).

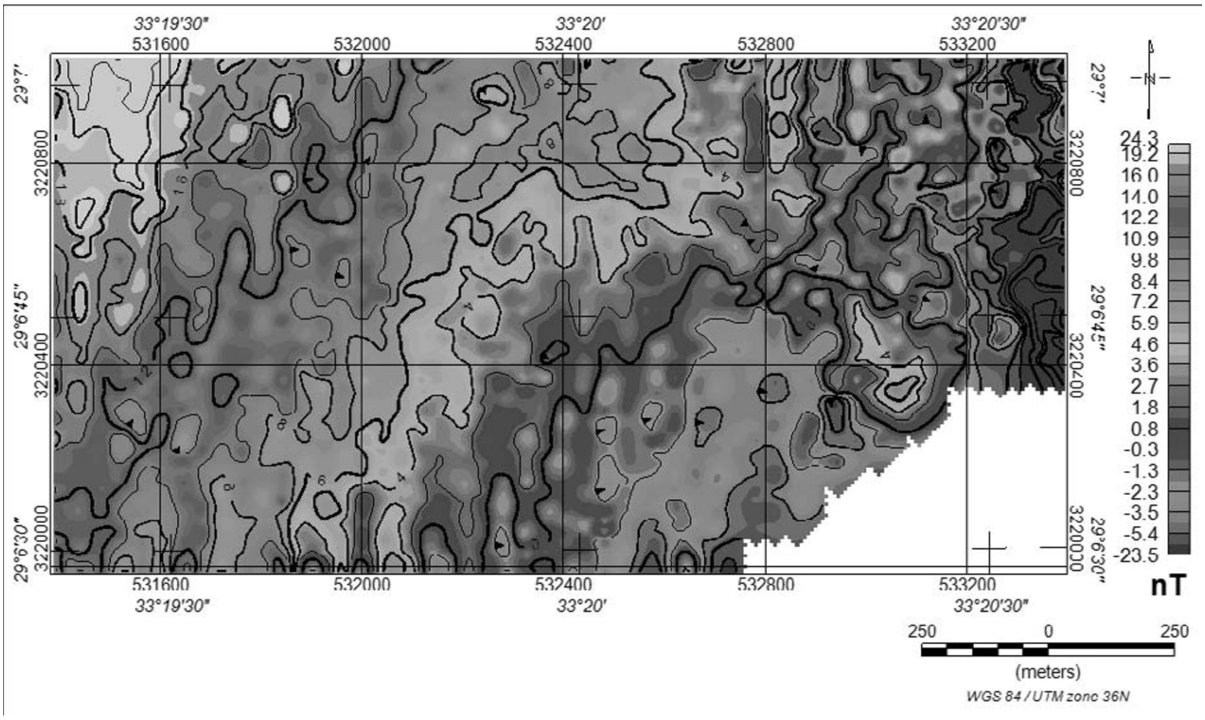

Fig. 5. Reduced to the pole magnetic map of the Abu-Rodaym area. C.I. = nT.

The RTP technique is the best method and more commonly used for removing magnetic distortion. The resulting map shows a direct correlation between magnetic highs and their causative sources. It can only be applied to data that were acquired at magnetic latitudes greater than approximately 20° north or south. The total intensity magnetic contour map (Fig. 4) of the study area, reduced to the north magnetic pole of the Earth, is shown in Fig. 5.

6. Filtering of the Magnetic Data

Filtering the magnetic data is an essential process prior to analysis and interpretation. The objective of the filter is to condition the data set and to render the resulting presentation in such a way as to make it easier to interpret the significance of anomalies in terms of their geological sources (Bird, 1997). Therefore, the most effective way to filter the data is with an understanding of the geologic control and the desired filtered results. Several filtering techniques can be performed in the frequency domain. However, one of the most traditional filters, used in the potential field, is the separation of long (deep), and short (shallow), wavelength anomalies. The success of this technique depends on the proper choice of cut-off wavelength used in the filter design. The cut-off wavelengths, and information about the contribution of the short and long wavelengths in the spectrum, can be obtained from the calculated radially-averaged power spectrum of the data.

Spectral analysis of the magnetic anomaly field, however, would indicate an ensemble average depth to the different sources of anomalies and, thus, would help to reveal a possible magnetic horizon/layer within the crust (Rama Rao *et al.*, 2011). A two-dimensional power spectrum curve of the present RTP data (Fig. 6) shows two linear segments related to long, and short, wavelength components with frequency bands ranging from 0.6 to 4.4 cycle/km, and from 4.4 to 17 cycle/km, respectively (Figs. 7 and 8). Following Spector and Grant (1970), the slope of these two linear segments were used to estimate the average depth to the top of the deep-seated, and near-surface, magnetic source. These depths are average estimates for the entire area and do not reflect a resolved and quantitative topography of the basement surface. The frequency bands corresponding to these linear segments were used through the band-pass filter technique to produce the regional, and residual, magnetic component maps. Meanwhile, the higher-frequency signal, beyond these segments, was considered as noise and was eliminated from the data to enhance the signal-to-noise ratio.

7. Euler Deconvolution

Euler deconvolution is an automatic technique used for locating the source of a potential field, based on their amplitudes and gradients. The method was developed by Thompson (1982) to interpret 2D magnetic anomalies, and was extended by Reid *et al.* (1990) to be used on grid-based data. A magnetic field M and its spatial derivatives satisfy Euler's equation of homogeneity:

$$(x - x_o)\frac{\partial M}{\partial x} + (y - y_o)\frac{\partial M}{\partial y} + (z - z_o)\frac{\partial M}{\partial z} = -NM, \quad (1)$$

where $\frac{\partial M}{\partial x}$, $\frac{\partial M}{\partial y}$ and $\frac{\partial M}{\partial z}$ represent first-order derivatives of the magnetic field along the x-, y- and z-directions, respectively; and N is known as a structural index and related to the geometry of the magnetic source. For example, $N = 3$ for a sphere, $N = 2$ for a pipe, $N = 1$ for a thin dike, and $N = 0$ for magnetic contact (Reid *et al.*, 1990). Taking into account a base level for the regional magnetic field (B),

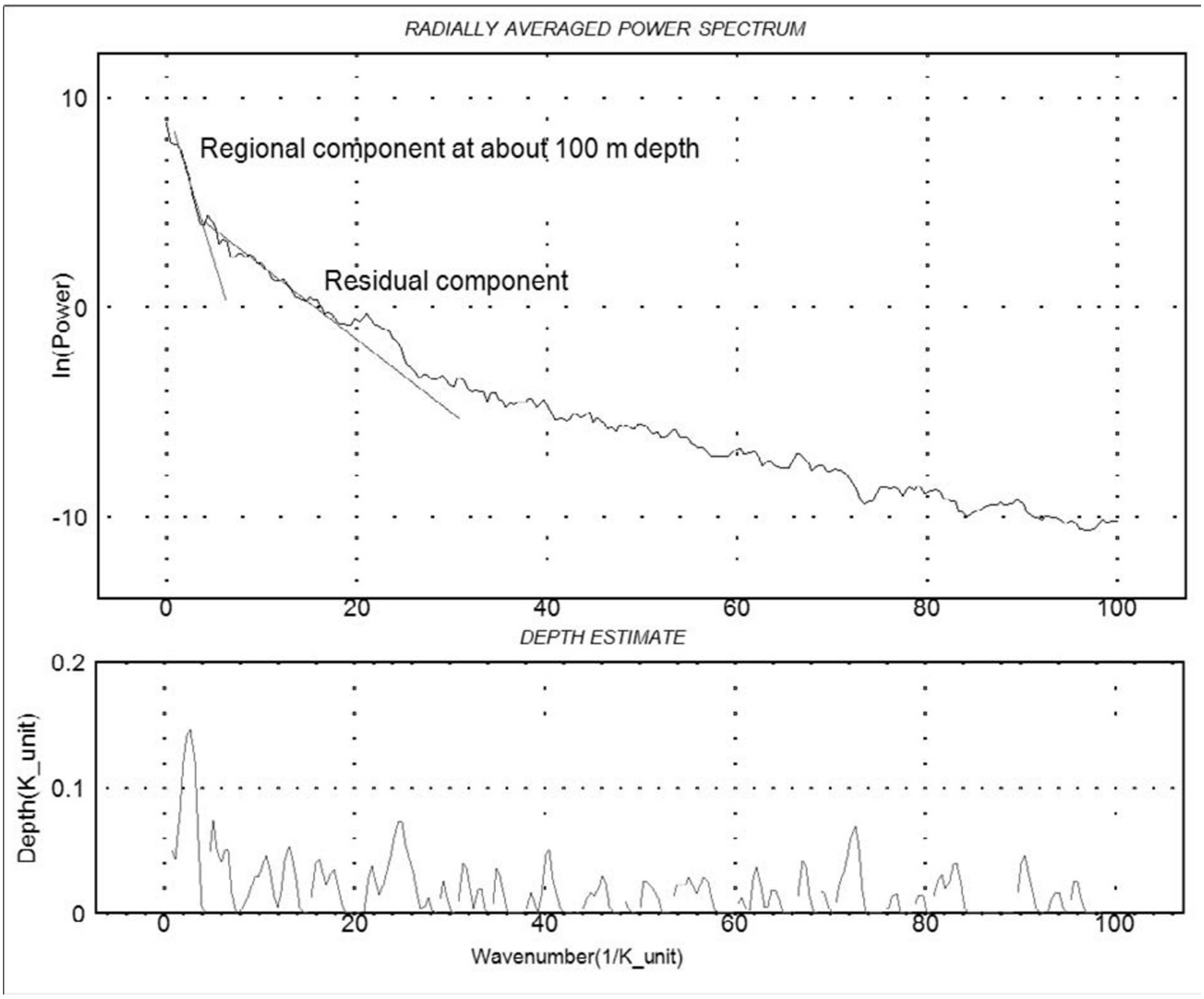

Fig. 6. Power spectrum curve and the estimated depths of the total intensity magnetic components of the Abu-Rodaym area.

Eq. (1) can be rearranged and written as:

$$x_o\frac{\partial M}{\partial x}+y_o\frac{\partial M}{\partial y}+z_o\frac{\partial M}{\partial z}+NB=x\frac{\partial M}{\partial x}+y\frac{\partial M}{\partial y}+z\frac{\partial M}{\partial z}+NM. \quad (2)$$

Assigning the structural index (N), a system of linear equations can be obtained and solved for estimating the location and depth of the magnetic body. Using a moving window, multiple solutions from the same source can be obtained. Good solutions are considered to be those that cluster well and have small standard deviations (Thompson, 1982; Reid *et al.*, 1990). Selection of the appropriate structural index is very important to obtain the correct depth solutions. However, the estimated horizontal location is independent of the structural index (Barbosa *et al.*, 1999), which means that there is no ambiguity with regard to the structural location. In this paper, we applied the method using the structural index ($SI \approx 0$) of contact or step (Thompson, 1982; Reid *et al.*, 1990), since the main objective is to map the faults and contacts. Despite generating scattered solutions, using a structural index very near to zero leads to a better estimation of depth and location of the contact/fault. After separating the regional component from the RTP map, the Euler deconvolution map (Fig. 9) was used to delineate the deep-seated structures from the regional-component map.

8. Results and Discussions

The interpretation of magnetic data of the study area is mainly carried out on the RTP magnetic map (Fig. 5), the regional component of deep-seated sources, and the Euler deconvolution maps (Figs. 7 and 10), which yield good information about the subsurface settings. The RTP magnetic map shows a gentle change in the magnetic field. This variation in the magnetic field of the RTP map is so steady and set in order of about 47.8 nT.

Depending upon the magnetic maps, the RTP regional and the RTP residual components (Figs. 7 and 8), and the Euler deconvolution map (Fig. 9), the following results can be obtained. The Abu-Rodaym area is intersected by three sets of faults, shown in Fig. 10. Two sets represent normal faults, with one trending in the N-S and the other trending in the NW-SE. The third set represents a group of strike-slip faults trending mainly towards the NE-SW direction.

These sets of faults were mapped using different rules and signatures of mapping faults from the magnetic data. Some of these rules used in mapping these faults depend on the following considerations: the contacts between any two different textures; the contact between any two different magnetic gradients; steep and gentle gradients that reflect

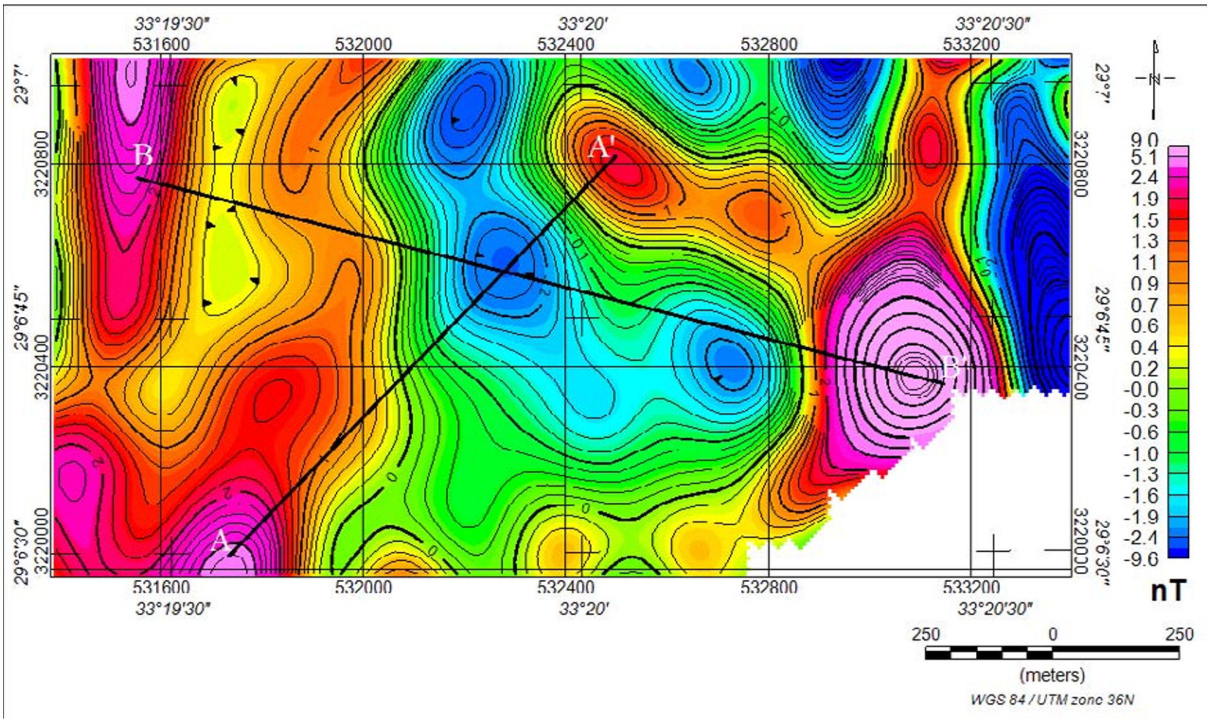

Fig. 7. Regional reduced to the pole magnetic map of the study area. C.I. = nT.

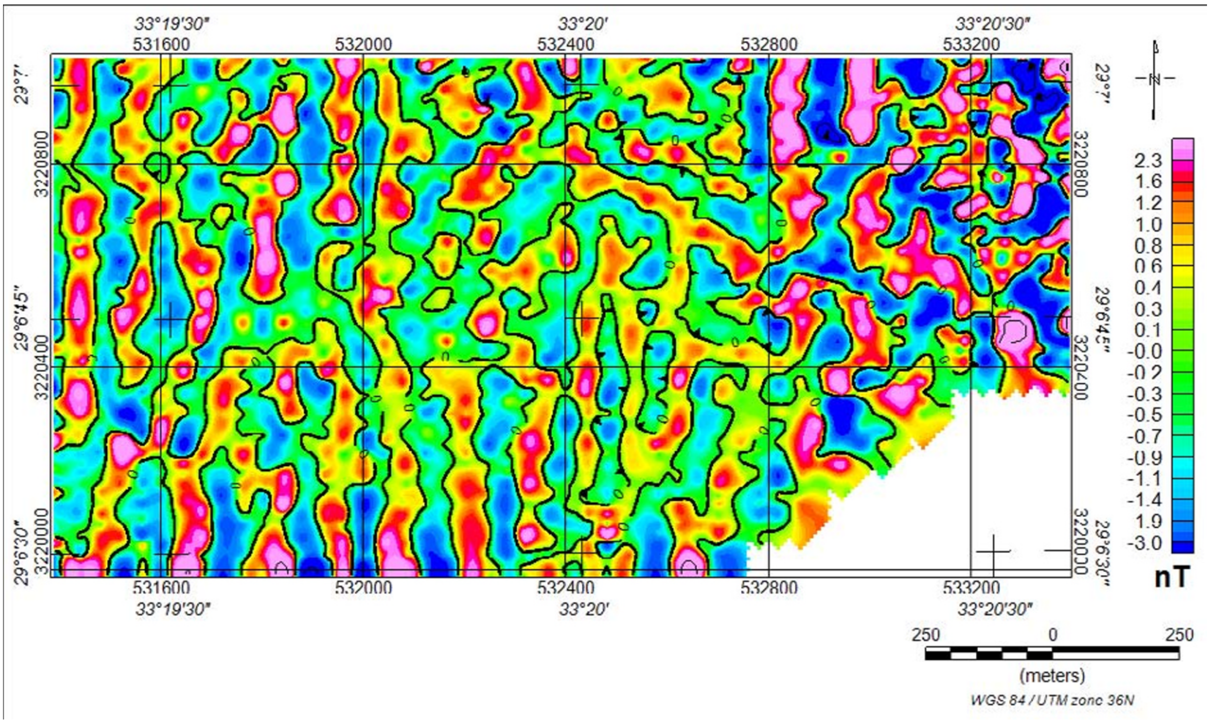

Fig. 8. Residual reduced to the pole magnetic map of the study area. C.I. = nT.

shallower, and deeper, magnetic blocks; sharp dislocation, or bends, in magnetic contour lines, especially if this is in the 90° range; the difference in magnetic intensities along a contact or lineament; and the relative positioning of similar magnetic anomalies, both in size and amplitude, that suggests a fault with a horizontal displacement only, rather than a vertical displacement (Rabie, 2011).

The existence of the first two sets of normal faults play the main role in creating graben structures G1, G2, G3, and G4 (Fig. 10), which occupy many parts of the study area, and represent sedimentary basins. Also, these basins seem to be open outside the area to the north and the south. Furthermore, the depth to the basement rocks at graben (G3), sited in the central part, is shallower than that under graben (G1) located at the eastern part of the study area. It is to be noted that these normal faults (Fig. 10), have

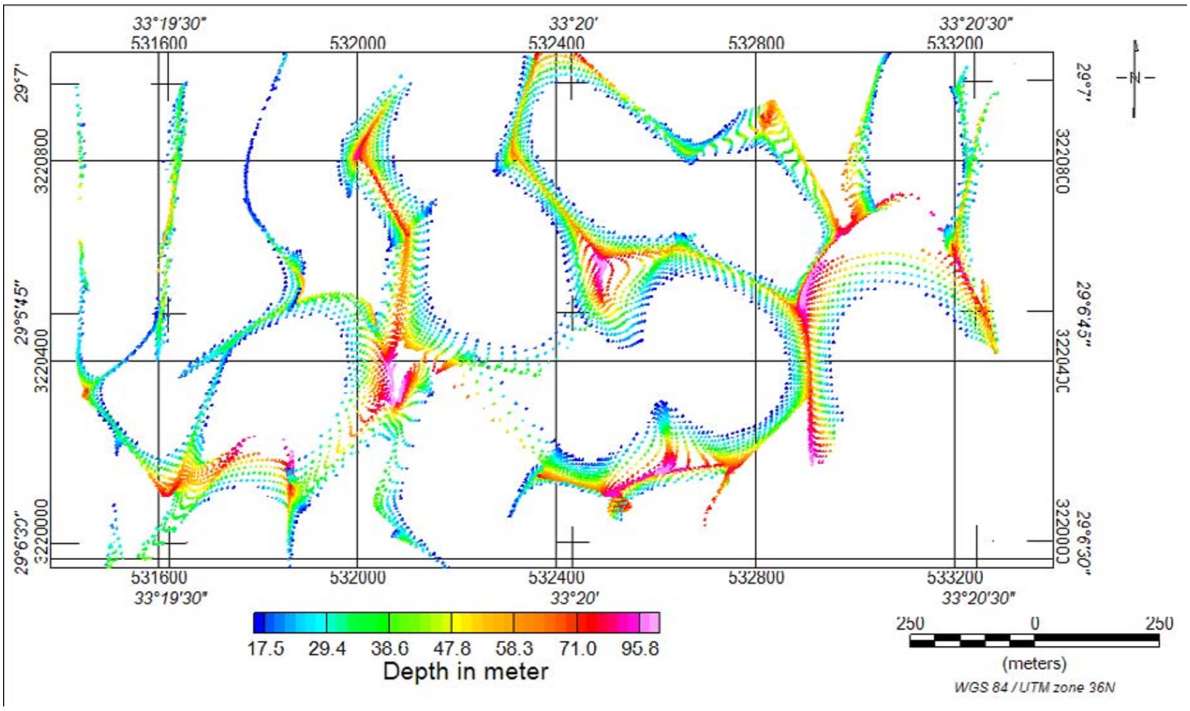

Fig. 9. Solution of the Euler method applied on the regional RTP magnetic map reflecting the deep-seated structural trends with a structural index = 0 (contact model). Black dotted lines indicated the geological contact.

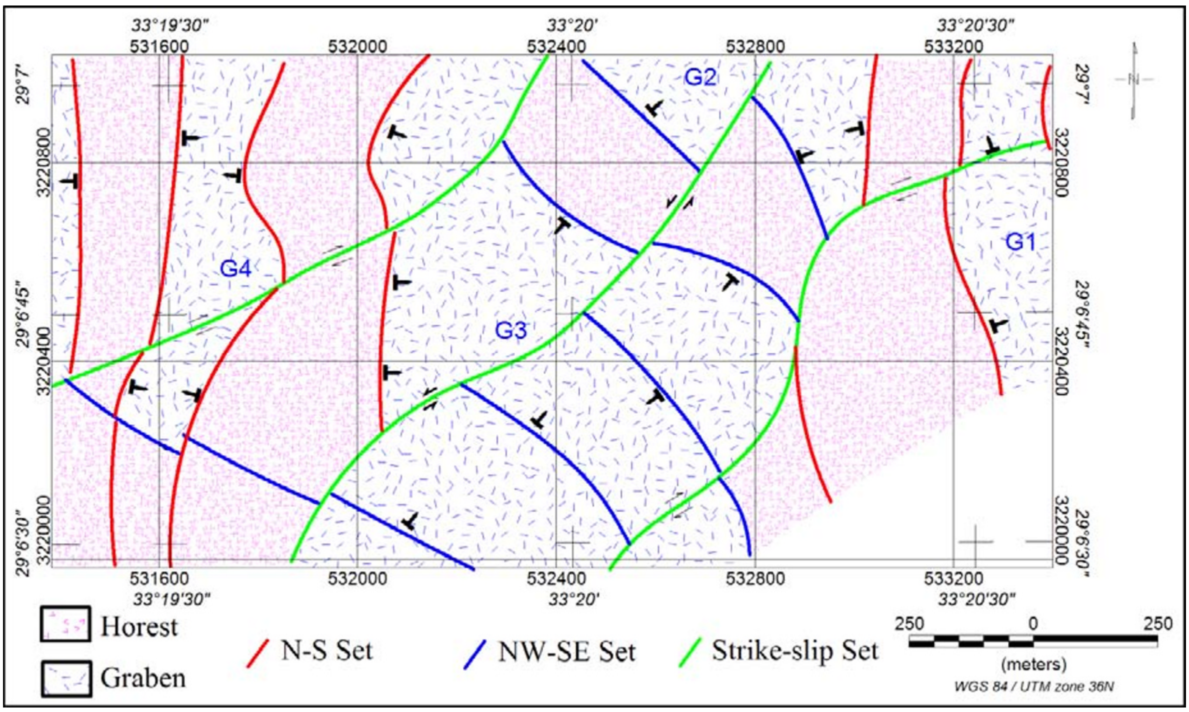

Fig. 10. Interpreted magnetic basement tectonic map of the study area.

been suggested to be of Miocene age, and parallel to the two complementary shear fractures of the Suez and Aqaba fault trends of Oligo-Miocene age (Said, 1990).

Considering the increasing thickness of the sedimentary succession in the study area, where the graben structures exist, the probability of the existence of groundwater bearing aquifers in these localities can be considered fair. These localities can be regarded as suitable basins in which groundwater aquifers could occur within the lower sandstone series, or the Abu-Thora formation. The best locations to drill for groundwater are at the boundaries of these grabens within the fault plane that surround these structures, because a fault plane always represents weak and open paths for groundwater, in this part of the Southeastern Sinai. Accordingly, it is logical to assume that such broad magnetic anomalies shown on the regional magnetic map (Fig. 7) can

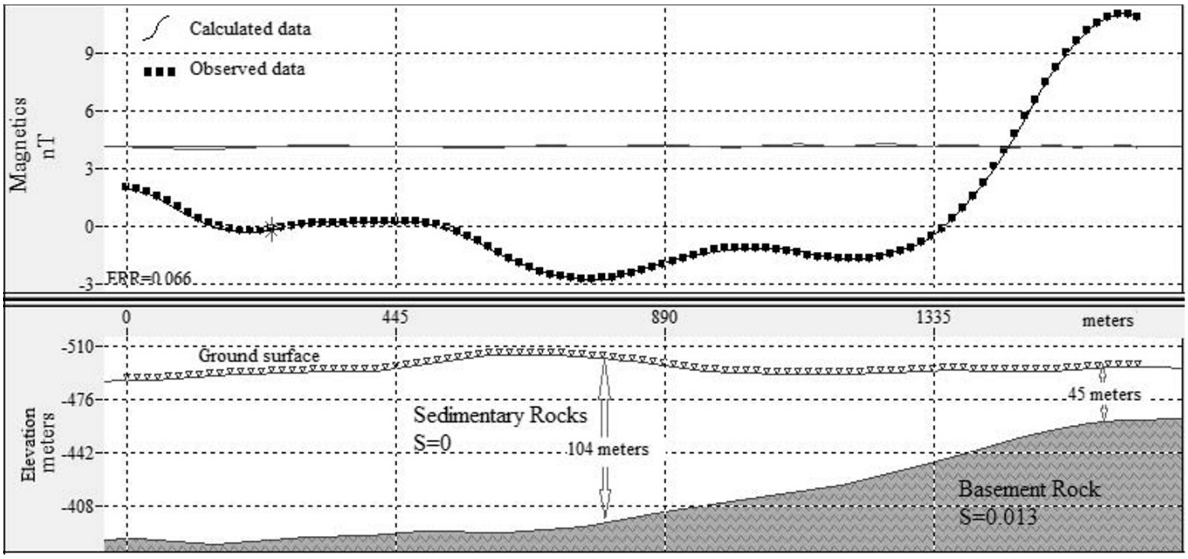

Fig. 11. 2D magnetic modelling of the profile (A–A′).

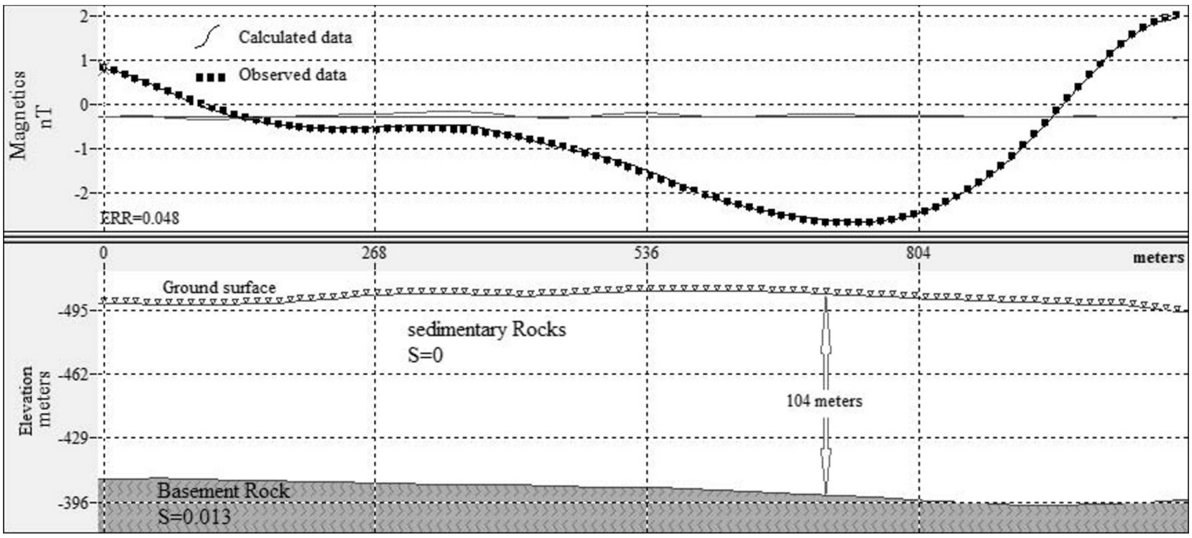

Fig. 12. 2D magnetic modelling of the profile (B–B′).

be related to basement rocks rather than any magnetic intrusion.

9. Magnetic Modelling

In order to calculate the depths to the basement surface, and to determine its susceptibility in the study area, two intersected profiles, (A–A′) and (B–B′), were applied on the regional reduction to the pole magnetic map using the GM-SYS program (Fig. 7).

Profile (A–A′) is about 1670-m long, and is directed from the northwestern corner to the southeastern part of the study area. The magnetic model of profile (A–A′) shows a remarkable variation in the thickness of the sedimentary rocks of the study area. It has a minimum thickness value of about 45 m at the end of the profile and a maximum of about 104 m at its central part (Fig. 11). The other model (B–B′) is directed from the SW to the NE direction and covers a length of about 1050 m. This model (Fig. 12) shows that the surface of the basement rock is inclined to the northeast direction, and the thickness of the sedimentary rocks varies consequently from about 90 m southward to about 105 m at the central part of the area under the point of intersection between the two models over the graben G3.

These two models emphasize that the magnetic variations in the basement rocks are mainly related to the variation in depth to the top of the different basement blocks, rather than its lithological composition, because it reflects the same value of magnetic susceptibility of about 0.013 (SI units).

10. Conclusions

The ground magnetic survey that was conducted in the Abu-Rodaym area has yielded good information about the subsurface structures, and their gross framework, which did not show any evidence on the surface. It reveals that the study area is intersected by three sets of faults trending entirely in the N-S and NW-SE directions. These two faults are considered as normal faults. The third set, trending in the NE-SW direction, are considered as strike-slip faults.

The results of 2D magnetic modelling indicated that, the depth to the surface of the basement rocks varied from 45 m to about 110 m, and proved that the variation in the magnetic field in the area was caused only by the striking faults rather than the variation in the lithological constituents of the basement. The study is characterized by graben structures, which represent suitable places to drill for groundwater-bearing aquifers, but carrying out a detailed ground geoelectrical survey over these graben locations is recommended in order to locate probable aquifers by following up the resistivity variation of the different rocks.

Acknowledgments. The authors thank the Exploration Division of the Nuclear Materials Authority (NMA) for providing the proton precession magnetometer (model PMG-1) and the Geosoft Oasis Montaj software package that was used for processing and mapping the magnetic data. The authors also appreciated the input of Dr. Ahmed A. Ammar, Dr. El-Sayed M. El-Kattan, and Dr. Baher M. Gheith, Professors of Applied Geophysics for supporting and reviewing this manuscript.

References

Al Shami, A. S., Studies on Geology and Uranium Occurrences of Some Paleozoic Rocks, Wadi Allouga Area, Sinai, Egypt, M.Sc. thesis, Zagazig University, Egypt, 1994.

Al-Shami, A. S., Structural and Lithological Controls of Uranium and Copper Mineralization in Um Bogma Environs, Southwestern Sinai, Egypt, unpublished Ph.D. Thesis, Faculty of Science, Mansoura University, 2003.

Barbosa, V. C. F., J. B. C. Silva, and W. E. Medeiros, Stability analysis and improvement of structural index estimation in Euler deconvolution, *Geophysics*, **64**, 48–60, 1999.

Barron, T., The Topography and Geology of the Peninsula of Sinai (Western Portion), Cairo: National Printing Department, 1907.

Bird, D., Interpreting magnetic data: Geophysical corner, EXPLORER, AAPG and SEG, May, 1997.

Dobrin, M. B. and C. H. Savit, *Introduction to Geophysical Prospecting*, 867 p, McGraw-Hill Book Co., New York, 1988.

El Rakaiby, M. I. and I. E. El Aassy, Structural interpretation of Paleozoice Mesozoic rocks, southwestern Sinai, Egypt, *Ann. Geol. Surv. Egypt XVI*, 1990.

Geosoft Inc, Oasis Montaj software package. Mapping and Processing system, Ontario, Canada, 2007.

Kora, M., The Paleozoic Outcrops of Um Bogma Area, Sinai, unpublished Ph.D. Thesis, Faculty of Science, Mansoura University, Egypt, 1984.

Mekonnen, T. K., Interpretation and Geodatabase of Dykes Using Aeromagnetic Data of Zimbabwe and Mozambique, M.Sc. Thesis, 80 p, ITC, Delft, the Netherlands, 2004.

Paterson, J. R. and C. V. Reeves, Application of gravity and magnetic surveys: The Stateof-Art, *Geophysics*, **50**, 2558–2585, 1985.

Rabie, M. A., Ground Geophysical Investigations for the Appraisal of Economic Minerals in Abu Rodaym Area, Southwestern Sinai, Egypt, Ph.D. Thesis, 143 p, Damietta University, Egypt, 2011.

Rama Rao, Ch., R. K. Kishore, V. Pradeep Kumar, and B. Butchi Babu, Delineation of intra crustal horizon in Eastern Dharwar Craton—an aeromagnetic evidence, *J. Asian Earth Sci.*, **40**, 534–541, 2011.

Reid, A. B., J. M. Allsop, H. Granser, A. J. Millet, and I. W. Somerton, Magnetic interpretation in three dimensions using Euler deconvolution, *Geophysics*, **55**, 80–91, 1990.

Said, R., *The Geology of Egypt*, 734 p, A.A. Balkema, 1990.

Spector, A. and F. S. Grant, Statistical models for interpreting aeromagnetic data, *Geophysics*, **35**, 293–302, 1970.

Thompson, D. T., "EULDPH" A new technique for making computer-assisted depth estimates from magnetic data, *Geophysics*, **47**, 31–37, 1982.

H. Aboelkhair (e-mail: h.aboelkhair@du.edu.eg) and M. Rabei